2009

Improving Efficiency in a Campus Chilled Water System Using Exergy Analysis

Justin M. Harrell
Southern Illinois University Carbondale

James A. Mathias
Southern Illinois University Carbondale, mathias@engr.siu.edu

Recommended Citation
Harrell, Justin M. and Mathias, James A. "Improving Efficiency in a Campus Chilled Water System Using Exergy Analysis." (Jan 2009).

Improving Efficiency in a Campus Chilled Water System Using Exergy Analysis

Justin M. Harrell, PE
Associate Member ASHRAE

James A. Mathias, PhD, PE
Associate Member ASHRAE

ABSTRACT

This paper evaluates the central chilled water system of the Southern Illinois University Carbondale (SIUC) campus using exergy-based cost accounting to quantify the magnitudes and cost impacts of internal losses with the goals of maximizing chiller capacity utilization and minimizing the unit cost of delivered chilled water. Two independent systems, each comprised of a primary-secondary-tertiary distribution network and cooled by a 12,300 kW (3,500 RT) steam-turbine-driven centrifugal chiller, were modeled as control volume networks using steady-state rate balances for energy, exergy, and cost. An extensive set of measurements, collected over the 2006 cooling season, was used as the input data for the models. Results show that while the steam turbines are the largest source of exergy destruction, mixing in the distribution loops is the dominant source of exergy unit cost at low cooling loads, and refrigeration cycle losses dominate costs at high loads. Recommendations include: (1) Convert the chilled water distribution to an all-variable-speed, direct-coupled configuration; (2) During low cooling loads use only one chiller; (3) During high cooling loads, increase the flow rate of water through the evaporators; (4) Favor speed control over inlet guide vanes for capacity modulation; (5) Better insulate steam piping; and (6) Consider replacing the steam turbines with variable speed motors.

INTRODUCTION

The Carbondale campus of Southern Illinois University (SIUC), as part of a campus-wide energy efficiency initiative, began a study in April 2006 of the campus central chilled water system, which was responsible for approximately one-quarter of the total annual utility expenditures in 2005. Of the chilled water production expenditures, steam accounted for 61% of the cost, maintenance for 16%, and electricity and water for 12% each. Due to significant escalation in coal and electricity rates, the cost of chilled water production had increased 33% by 2007. In addition to these high costs, the system was not achieving its full capacity despite comfort complaints and humidity problems that indicated unmet cooling load. These findings indicated that there were significant opportunities to improve the performance and efficiency of the chilled water system.

The central chilled water system consists of two independent primary-secondary-tertiary distribution networks, each cooled by a large vapor compression refrigeration plant powered by a steam turbine. Each plant is rated for 12,300 kW (3,500 RT) of cooling and 21,700 kg/hr (47,850 lbm/hr) of steam consumption. The central chilled water system provides nearly all the cooling on campus except for student housing and some buildings with unique cooling requirements such as the basketball arena. The two vapor compression chiller plants that comprise the chilled water system are located near the west and south sides of campus; consequently they will be referred to as the West and South chillers.

Others have studied and improved refrigeration systems through modeling and analysis of experimental data. Hyman and Little (2004) analyzed the central chilled water system of the University of California Riverside (UCR) campus which also consisted of a primary-secondary-tertiary pumping network. Due to inconsistent design standards over the years, some of the building (tertiary) loops were piped in series with the campus distribution (secondary) loop while others were connected with decoupling bypasses. This created negative pressure differences across the distribution mains at buildings

remote from the chiller plant while, at buildings near the chiller plant, excessive positive pressure differences caused water to short-circuit back to the plant. These problems contributed to "low delta-T syndrome" which occurs when the temperature difference between the water supplied by the chiller plant and the water returning from the distribution network is noticeably lower than the designed temperature difference. Low delta-T syndrome limits the chiller capacity, resulting in inadequate cooling to the buildings served by the system. To alleviate the problems, some of the recommendations included installing variable frequency drives (VFDs) to run the building pumps at reduced speeds, hydraulically decoupling the buildings that were piped in series, and installing pressure-independent control valves at locations close to the plant to eliminate leaking through the control valves.

Taylor (2002) reviewed other causes of the low delta-T syndrome in central chiller systems including improper selection of coils and control valves, coils piped backwards, and short-circuiting of water due to improper control of building bypass flow. Some solutions suggested to alleviate low delta-T syndrome were the use of a reset control to modulate the return water temperature setpoint in response to building supply temperature, placement of a check valve in the building bypass to block short-circuit flow, and switching to variable-flow, primary-only pumping.

Klein et al. (1988) studied a university chiller system, nearly identical to that of SIUC, consisting of two 12,300 kW (3,500 RT) centrifugal chillers driven by condensing steam turbines and rejecting heat through cooling towers equipped with two-speed fans. They used mechanistic models of chiller system components to identify key parameters using a least-squares fit of model output to collected data. The combined component models approximated the actual operating costs within 2% and resulted in the development of optimal control maps for inlet guide vane position and cooling tower fan speed over the range of typical cooling loads and wet-bulb temperatures.

Braun (1989) developed a complex component-model-based optimization algorithm from which a series of heuristic rules for optimal control were derived. These rules were then used to develop a simpler system-based model suitable for developing optimal control maps or for online chiller optimization. The system-based model used chiller load and wet-bulb temperature as the independent variables and optimized five control parameters using a quadratic cost function.

Hartman (2001) proposed a method of optimal control for chiller plants using demand-based control rather than control laws developed from mechanistic or empirical component models. The system is called demand-based because it optimized the power inputs with respect to the load without explicitly controlling system variables, such as chilled water temperature, with local control loops. Chiller systems using this type of control must be all-variable speed and directly-coupled to the loads without the use of decoupling bypasses.

Hartman claims overall power reductions of 30%-50% are achievable over typical performance.

A thermodynamic approach to modeling chiller systems has been proposed by Gordon and Ng (2000) for predictive, diagnostic, and optimization purposes. Their studies of chiller systems revealed three principle causes of inefficiencies: internal dissipation due to fluid and mechanical friction, entropy generation during heat transfer, and heat leaks between thermal reservoirs. They developed a steady-state multiple linear regression model for coefficient of performance (COP) given inputs of chiller load, and water temperature entering the condenser and evaporator. The regression results in three parameters which quantify the three causes of irreversibility.

Rosen and Dincer (2004) advocated the use of exergy analysis in the study of thermal systems, emphasizing that energy analysis alone is often inadequate in assessing performance improvement. Exergy analysis, which combines conservation of mass and energy with the second law of thermodynamics, quantifies the maximum potential of a system to do work were it to fall into equilibrium with the larger surrounding environment. Exergy analysis is useful in efficiency studies because it identifies the true locations and magnitudes of losses within the system, and reveals the maximum available performance improvement. Exergetic efficiency is always between zero and unity and consequently can be used to compare processes of different types on a common basis, unlike energy efficiency and COP. Rosen and Dincer applied exergy analysis to industrial steam process heating (2004). Rosen et. al (2004) applied exergy analysis to a district heating and cooling system with cogeneration, developing expressions of both energy and exergy efficiency for the components as well as the system as a whole.

The fundamentals of thermodynamic modeling using steady-state rate balances on control volumes were covered by Moran and Shapiro (2000). They also advocated the use of exergy analysis in understanding thermal systems and developed expressions for exergetic efficiency and exergy-based cost accounting.

This paper provides a detailed description of the central chilled water system of the SIUC campus and reports on the data acquisition, modeling process, and exergy analysis. The data acquisition portion describes the measurements taken and the quality control procedures used to create a steady-state data set for modeling that is representative of the range of the chiller system operation. The construction of the system model, based on steady-state, control-volume rate balances for energy, exergy, and cost, is described. Emphasis is placed on using exergy analysis to identify the system components that greatly contribute to below-rated cooling capacity and high operational costs. The results of the paper are valuable as they highlight the usefulness of exergy analysis in understanding and improving energy utilization in chiller systems. The results for this central chilled-water system should be appli-

cable to many other large central chilled-water systems currently in operation.

SYSTEM DESCRIPTION

The West chiller serves eleven academic buildings that consist of classrooms, research laboratories, and office space with a gross area of 96,618 m² (1,040,000 ft²). The South chiller serves nine buildings that are academic, administrative, athletic, and commercial with a gross area of 115,152 m² (1,239,486 ft²). Both chillers suffer from excess load relative to chiller capacity; the West and South chillers can serve only 73% and 67% of the design load, respectively, which results in comfort complaints and excessive moisture in some buildings.

Chilled Water Distribution Subsystem

Distribution of water in both chiller systems is accomplished with a primary-secondary-tertiary loop subsystem, shown in Figure 1. The ladder shape of the piping formed by the distribution mains and bypasses indicates a direct-return system, where flow in the mains reduces downstream of each building. The schematic shows simplified building loops where all the cooling coils in that building are represented by one coil. The primary loop circulates water through the West and South chillers at a constant, nominal rate of 312 L/s (4950 gpm) and 442 L/s (7000 gpm), respectively. Each chiller loop uses three constant-flow pumps in parallel to achieve this, and in typical operation, two pumps are running, with the third in standby.

The secondary, or distribution, loops pull water from the primary loops using three variable-speed pumps in parallel and the West and South distribution loops circulate it around campus at a nominal peak rate of 479 L/s (7600 gpm) and 580 L/s (9200 gpm), respectively, to each building service point and back to the plant. The primary-to-secondary loop flow ratios of the West and South chillers are 65% and 76%, respectively. The primary and distribution loops of each chiller are decoupled using a full-bore open bypass such that the speed and direction of the flow in the bypass is determined solely by the relative flows in each loop. The distribution loop pumps are located adjacent to each chiller and are powered by VFDs, which are controlled to maintain an adjustable differential pressure setpoint between supply and return at certain buildings located near the end of the loop. As campus cooling load increases, the buildings require more chilled water flow, reducing the differential pressure across the distribution loop mains causing the distribution pumps to speed up to meet the demand.

When campus building loads and distribution loop flow requirements are low, the bypass flow will be in the direction of supply to return until the pump speed exceeds the primary-to-secondary flow percentages indicated. As the distribution loop flow increases beyond this point, the bypass flow will stop and then reverse direction. In the former condition, the chiller experiences a reduced return water temperature relative to the distribution loop as cold supply water mixes with the return water before entering the chiller. In the latter condition, the distribution loop supply experiences a raised temperature relative to the primary loop as warm return water mixes with the supply water before exiting the plant.

The tertiary, or building, loops each have their own constant speed pump, except for the buildings where the chillers are located which take advantage of the proximity of the
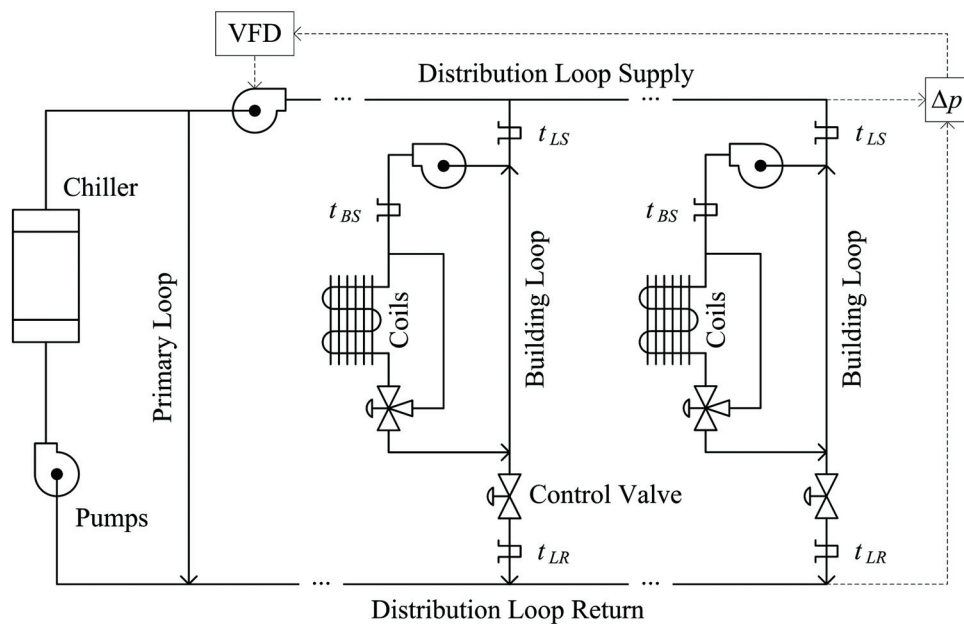

Figure 1   *Chilled water distribution subsystem schematic.*

distribution pumps. Like the primary-secondary interface, each building is decoupled from the distribution loop using a full-bore open bypass, however, chilled water flow to and from the distribution loop is regulated by a pneumatic control valve located in the return leg between the distribution return main and the building loop bypass.

Figure 1 also shows the locations of the three temperature sensors installed at each building to monitor (1) the supply temperature from the loop, t_{LS}; (2) the return temperature to the loop, t_{LR}; and (3) the supply temperature to the building, t_{BS}. The building control valves are modulated to maintain the loop return temperature at a high setpoint in order to mitigate the "low delta-t syndrome" that often plagues large chilled water distribution subsystems. Harrell (2008) describes the control scheme used to obtain a high loop return temperature coupled with a reset schedule to maintain minimum dehumidification capability.

Refrigeration Subsystem

The refrigeration subsystem consists of a single-stage centrifugal compressor, two flooded shell-and-tube heat exchangers, serving as the condenser and evaporator, and a throttling valve. The working fluid is R-134a. In both the evaporator and condenser, water flows through the tube side and refrigerant through the shell side. Refrigerant leaves the evaporator as slightly superheated vapor and leaves the condenser as subcooled liquid. The South chiller has two water passes in the condenser and evaporator, while the West chiller has two water passes in the condenser and three water passes in the evaporator.

Both chillers have the same maximum rate of cooling, but other ratings differ slightly due to the extra water pass in the West chiller evaporator. The West chiller compressor is rated for 2,031 kW (2,723 hp) at 5,476 rpm, yielding a rated COP of 6.06 (0.778 hp/RT). The South chiller compressor is rated for 2,071 kW (2,777 hp) at 5,480 rpm, yielding a rated COP of 5.95 (0.793 hp/RT).

The refrigerant liquid level in the condenser is regulated by a float that controls the operation of the globe-type throttling valve with a pneumatic actuator. Maintaining a fixed volume of liquid refrigerant in the condenser creates an integral subcooler. The condenser water supply cools this liquid volume on its initial pass and thus the entering water temperature is the primary factor that determines the extent of subcooling and the condensing pressure of the refrigerant. The evaporator is also partially flooded; however the level depends on the refrigerant charge and the boiling and condensation pressures. The evaporator pressure depends mainly on the leaving chilled water temperature, the primary control point in the chiller system, which is manually set to 6.7°C (44°F) and raised to 8.3°C (47°F) at the beginning and end of the cooling season when loads are light.

At a constant compressor speed, the temperature setpoint of the chilled-water supply is tracked using proportional-integral (PI) control and maintained under varying load conditions by modulating the compressor inlet guide vanes and diffuser throttle to control the chiller capacity. For part loads down to 50%, the guide vanes act alone; for loads below 50% down to 10%, the vanes and diffuser throttle work together to reduce the capacity by limiting the flow of refrigerant.

Compressor throttling and turbine load are reduced at part loads via automatic turbine/compressor speed reduction. The control is setup such that the compressor runs at maximum or rated speed when the water temperature entering the condenser is greater than 24.4°C (76°F) and runs at minimum speed when the temperature is at 1.7°C (35°F). The speed is linearly interpolated at intermediate temperatures. This control takes advantage of the reduction in required compressor lift associated with reduced entering condenser water temperature. Input power reduces cubicly, available pressure lift reduces quadratically, and refrigerant flow reduces linearly in proportion to the speed reduction. A reduced refrigerant flow due to compressor speed reduction allows the inlet guide vanes and diffuser throttle to operate in a more open position.

Steam Turbine Drive Subsystem

The power source for the compressors in each chiller plant is a five-stage condensing steam turbine. Turbines in both chiller plants are directly coupled to the compressors and are rated for 2,623 kW (3,518 hp) at 5,491 rpm and steam rate of 2.30 kg/MJ (13.6 lbm/hp-hr). Steam is provided by the coal-fired campus boiler plant in a saturated state between 830-860 kPag (120-125 psig). Figure 2 shows a schematic of the steam turbine drive subsystem.

The steam passes first through a differential-pressure, totalizing mass flow meter to record the amount of steam entering the chiller plant. Next, any condensate is removed with steam traps prior to entering the turbine. Subsequently, the steam flows into the turbine steam chest and steam ring. The turbine is an impulse design where steam is accelerated through rings of nozzles which direct steam jets into buckets on the perimeter of the rotor wheels. Turbine speed is measured using an optical encoder whose signal is compared to the speed setpoint generating an error signal that causes the governor to modulate valves regulating steam flow to the nozzles. The turbine speed is set based on entering condenser water temperature as described previously.

A small portion of the steam flow condenses in the turbine, collecting in the bottom of the casing where it drains by gravity into a receiving tank (not shown) and is pumped into the surface condenser. The large majority of the exhaust flow exits the top of the turbine and is directed to the top of the surface condenser. The turbine exhaust, condensate tank and the surface condenser are all interconnected and under a deep vacuum of typically 88-95 kPag (26-28 in. Hg). This vacuum is the condensing pressure of the steam and is determined mainly by the temperature of the entering condenser water. The surface condenser is a shell and tube heat exchanger with a single water pass where the steam condenses on the surfaces of the water tubes and collects in the hotwell below. Conden-
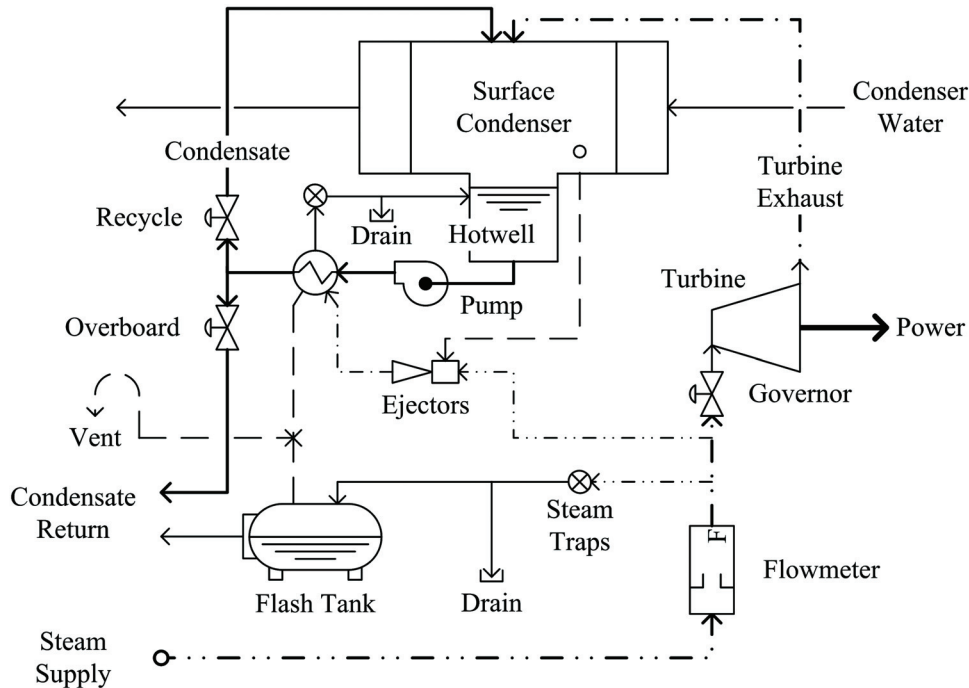
Figure 2 *Steam turbine drive subsystem schematic.*

sate is pumped from the hotwell at a constant rate of 7.6 L/s (120 gpm) and returned to the condenser through the recycle valve or returned to the steam plant through the overboard valve. The liquid level in the hotwell is maintained by a float control which operates the recycle and overboard valves in opposition to each other. The hotwell pump flow exceeds the steam flow of the turbine at rated conditions by approximately 25%, so a portion of the condensate is always recycled to the top of the surface condenser.

The auxiliary ejector portion of the subsystem is also shown, highly simplified, in Figure 2. The ejectors assist in maintaining the exhaust vacuum by removing any air that might leak in through minute gaps in seals and joints. The ejectors work by accelerating high pressure steam through a nozzle, creating suction on a pipe connected perpendicularly to the nozzle throat. There are three ejectors and the exhaust of each ejector enters a separate condenser where the liquid is removed by a float-type steam trap and the non-condensable gasses exit through a vent.

Heat Rejection Subsystem

The heat rejection subsystem consists of a constant-flow, pumped condenser water loop that absorbs heat from both the refrigerant condenser and steam surface condenser and rejects it to the environment using evaporative cooling towers. Both chiller plants are designed with a condenser water rate of 54 L/MJ (3 gpm/RT), equaling 662 L/s (10,500 gpm). Both chiller plants use multiple cross-flow induced-draft cooling towers with adjustable fan speed. The South plant uses six tower cells

each with a two-speed fan. The West plant uses two tower cells each with a VFD-controlled fan.

In the cooling towers, hot condenser water is sprayed from a header onto the tower fill which is designed to maximize the water surface area as it drips and splashes down toward the sump. The fan at the top of the tower pulls air in the sides of the tower through the dripping water. Approximately 1-2% of the condenser water evaporates into the air that then leaves the cooling tower at or very near saturation. The cooling is limited fundamentally by the ambient thermodynamic wet-bulb temperature, which is the temperature of adiabatic saturation. Because of the effect of condenser water temperature on the condensing pressures of both the refrigerant and the steam, the ambient wet-bulb temperature has a profound influence on the chiller operation and efficiency.

The cooling tower fans are controlled so that the temperature of the water exiting the tower sump will not drop below an adjustable setpoint when the outdoor wet-bulb temperature is low. The control schemes work differently in each chiller. At the West chiller, the two fans are controlled to obtain an exiting water temperature of 20°C (68°F). When the tower cannot achieve this due to high wet-bulb and/or high chiller load, both fans run at 100% speed. As the water temperature approaches the setpoint both fans slow down together using PI control to target the setpoint. If the water temperature continues to drop, the fans shut off completely. At the South chiller, the six fans are controlled in three sets of two with three speed steps: off, low, and high, where low speed is 50% of high speed. This arrangement gives the towers a total of seven levels of airflow.

The stages are implemented with two tower exit water temperature setpoints so that above the high setpoint, 22.2°C (72°F), all the fans are on high and below the low setpoint, 18.9°C (66°F), all the fans are off, with the intermediate stage transitions evenly spaced between the setpoints. A brief startup and shutdown delay is used to avoid short-cycling the fans.

In both chillers, an additional control measure is implemented to ensure that the entering condenser water temperature, and thus the condensing pressure and turbine speed do not drop too low. A cooling tower bypass valve is located between the cooling tower supply and return so that a portion of the condenser water may be diverted back to the condenser without being cooled by the tower. This valve opens at low loads and/or low ambient wet-bulb temperature should the condensing pressure drop below a minimum adjustable setpoint. The valve operates using PI control to accurately maintain the minimum condensing pressure setpoint of 517 kPag (75 psig).

Water evaporated in the cooling tower is replaced by city makeup water via float-controlled valves in the tower sumps. Water quality is monitored continuously in the loop and chemicals are automatically injected as needed to prevent the buildup of biofilms and scale on heat transfer surfaces. The water quality controller also monitors the concentration of solids in the water and periodically opens the blowdown valve, sending some of the water to the drain to be replaced by clean makeup water. Both the makeup and blowdown flows are recorded with totalizing turbo meters. A refund of sewer charges is obtained from the city for the makeup water that is evaporated and not processed by the sewer treatment plant.

SYSTEM MODELING

Data Collection

Data for both chiller systems were collected during the 2006 cooling season. Table 1 shows the available measurements that were collected and used for modeling. Most data were recorded automatically every five minutes through an automatic data collection system. Steam mass flow rate and cooling tower fan speed were recorded as part of a manual data log taken three times per week.

Hourly weather data were obtained from an automated weather station located less than 0.625 km (1 mi) from the chiller systems. The weather station samples data every ten seconds and averages the data over a one hour period and then archives the information. The weather station provided data of ambient dry-bulb temperature (°F), ambient barometric pressure (mbar), and ambient relative humidity (%). From these data, the thermodynamic wet-bulb temperature was calculated and used in conjunction with the barometric pressure to define the exergetic reference state for each hour.

After the data were collected, a procedure was followed to obtain steady-state data on an hourly basis. First, for the data that were recorded every five minutes, if there were not at least ten available records per hour, then all the data for that hour

Table 1. Data Collected for Modeling

Subsystem	Measurement	Unit
Chilled Water Distribution Subsystem		
	Primary Loop Flow Rate	gpm
	Evaporator Inlet Temperature	°F
	Evaporator Exit Temperature	°F
	Distribution Pump Speed	Hz
	Distribution Loop Supply Temperature (each building)	°F
	Distribution Loop Return Temperature (each building)	°F
	Building Loop Supply Temperature (each building)	°F
Refrigeration Subsystem		
	Evaporator Pressure (centerline)	psig
	Evaporator Temperature (centerline)	°F
	Condenser Pressure (centerline)	psig
	Compressor Discharge Temperature	°F
	Subcooler Exit Temperature	°F
Steam Turbine Drive Subsystem		
	Steam Mass Flow Rate (manually recorded)	lbm/hr
	Steam Supply Pressure	psig
	Surface Condenser Vacuum Pressure	in. Hg
	Hotwell Exit Temperature	°F
Heat Rejection Subsystem		
	Cooling Tower Exit Temperature	°F
	Condenser Exit Temperature	°F
	Surface Condenser Exit Temperature	°F
	Cooling Tower Fan Speed (manually recorded)	%

were unused. Next, if the standard deviation of the data collected throughout the hour was zero, then a communication problem in the data acquisition system was suspected and the entire hour of data, as well as the hour before and after, were unused. All the data for any hours during which the calculated evaporator cooling load indicated a chiller outage were rejected. Finally, the steady-state condition was defined using the chiller testing criteria of the Air-Conditioning & Refrigeration Institute (ARI) Standard 550/590-2003 (ARI, 2003) as a guide. Table 2 shows the tolerances of the ARI standard and those used. Hourly mean data qualified as steady-state if the maximum deviation from the mean within one hour did not exceed the tolerances shown. The steady-state requirements for the data of the South chiller were relaxed compared to the ARI standards to obtain approximately equal-sized data sets

Table 2.   Steady-State Data Tolerances

Measurement	ARI 550/590 Tolerance	Tolerance Used	Chiller
Water Flow Rate of Primary Loop	± 5% of Rated Value	± 23 L/s (365 gpm) (± 5% of Typical)	Both
Temperature of Chilled Water Exiting Evaporator	± 0.3 °C (0.5 °F)	± 0.3 °C (0.5 °F)	Both
Temperature of Condenser Water Exiting Cooling Tower	± 0.3 °C (0.5 °F)	± 0.3 °C (0.5 °F)	West
		± 0.6 °C (1.0 °F)	South
Heat Transfer Rate Within Evaporator	± 2% of Full Load Value	± 246 kW (70 RT) (± 2% of Full Load)	West
		± 492 kW (140 RT) (± 4% of Full Load)	South

for each chiller. The two-speed fans of the South chiller cooling tower caused greater fluctuations in the condenser water temperature as compared to the VFD-controlled fans of the West chiller cooling tower. Data used for modeling was selected from the steady-state data set for those hours during which steam mass flow and cooling tower fan speed measurements from the manual data log were available. Data selected for the modeling spanned the range of operation of the chillers throughout the cooling season and is shown elsewhere (Harrell, 2008). The data show that the South chiller was typically much more heavily loaded than the West chiller and that neither chiller achieved its full rated capacity. The West chiller model data set was fairly representative of the load profile, while the South chiller model data set was biased toward the higher end of the load profile.

Energy Modeling

Energy conservation was applied to an interconnected series of steady-state control-volume rate balances at three levels: (1) the entire chiller system; (2) each of the four chiller subsystems: (a) chilled water distribution, (b) refrigeration, (c) steam turbine drive, (d) heat rejection; and (3) each major subsystem component, such as the evaporator, compressor, etc. Energy conservation applied under steady-state conditions guarantees that all entering energy also leaves the system as shown in Equation 1, where changes in kinetic and potential energy are assumed negligible.

The signage in Equation 1 indicates that the positive direction for heat and mass transfer is into the system, and the positive direction for power transfer is out of the system.

$$0 = q - P + \sum_i m_i h_i - \sum_e m_e h_e \qquad (1)$$

Heat transfer into the system occurs at the cooling coils and with the steam supply flow. Heat transfer out of the system occurs at the cooling tower and with heat losses from the high pressure steam piping between the mass flow meter and the turbine. Other than at these locations, all of the modeled control volumes were assumed to be adiabatic. All throttled flow was assumed to be isenthalpic. Complete fluid states and energy transfers were calculated from the available data shown in Table 1.

The heat transferred from the chilled water distribution subsystem was calculated from the flow rate and temperature difference of the chilled water across the evaporator. Pumping power was derived from nameplate ratings and the recorded VFD speed for the distribution pumps. All pumping power was dissipated as friction heating of the chilled water and subtracted from the evaporator heat transfer to calculate the total heat transfer at the cooling coils of the buildings. For each chiller model, all the building loops served were aggregated into a single representative building loop with a single cooling coil.

The refrigeration subsystem was modeled by determining the refrigerant flow rate through an energy balance around the evaporator using the known enthalpies of the chilled water and refrigerant at the inlet and exit of the evaporator and the known chilled water flow rate. The power input to the compressor was found using the calculated refrigerant flow rate and the enthalpy difference across the compressor, the enthalpy inlet to the compressor being the same as that exiting the evaporator. The heat transferred from the refrigerant in the condenser was calculated from the refrigerant flow rate and enthalpy difference across the condenser, which was determined from the measured temperatures and condenser pressure. The refrigerant enthalpy at the exit of the condenser remained constant through the valve and was also used as the enthalpy entering the evaporator. As only centerline pressure measurements were available for the evaporator and condenser, pressure drops in the heat exchangers were neglected.

The steam turbine drive subsystem was modeled by first calculating the heat rejected to the condenser water in the steam surface condenser using the recorded water temperatures and the water flow rate calculated from the refrigerant condenser energy balance. The steam flow rate through the turbine was found from the surface condenser energy balance using the measured condensing vacuum pressure and hotwell exit temperature. Simultaneously, the enthalpy of the partially-condensed steam at the exit of the turbine was calculated by setting the turbine power output equal to the compressor power input, neglecting minor friction losses. The enthalpy of the steam supplied to the turbine was determined by the saturated vapor condition and measured pressure. The flow rate of trapped condensate due to heat loss from the high pressure steam piping was calculated by subtracting the calculated turbine steam flow rate and the design ejector flow rate from the measured total steam supply flow.

The heat rejection subsystem was modeled by summing the heat transfer to the condenser water from the refrigerant and steam condensers and the minor friction heating due to the condenser water pumps and rejecting this energy via evaporation in the cooling tower. The cooling tower bypass flow rate was calculated from an energy balance using the measured and calculated water temperatures. The evaporation rate was determined from the heat rejection rate and the latent heat of vaporization at the log-mean temperature of the tower water and atmospheric pressure. Makeup and blowdown rates were determined using the annual average evaporation-to-makeup ratio based on the totalized flow from the water meters. Total heat rejection was equal to the heat lost by the cooling tower water plus the cooling tower fan power, which was dissipated as friction heating of the air.

Exergy Modeling

After all the mass flows, energy flows, and fluid states were determined, steady-state exergy balances were performed for the same control volumes as the energy analysis. In the exergy analysis, all control volumes were assumed to be adiabatic and to have negligible changes in kinetic and potential energy, as shown by Equation 2. The object of the analysis was to determine within each process the exergy destruction rate, E_d, which is the rate of loss of available work due to entropy generation. The specific flow exergy, e_f, is a fluid property analogous to specific enthalpy, h, used in the energy balance, Equation 1. Specific flow exergy, defined in Equation 3, represents the available work per unit mass contained in the fluid relative to its *dead state*, denoted by the subscript, o, in equilibrium with the surrounding environment. The term, $T_o(s-s_o)$, in Equation 3 equals the energy per unit mass that would account for a drop in entropy from the fluid state to the dead state if heat were transferred isothermally and reversibly from the fluid to the environment at the dead state temperature, T_o. Since the fluid entropy cannot be lowered through a real adiabatic flow process, this quantity of energy is unavailable for recovery as work and is subtracted from the gross enthalpy difference between the fluid and its dead state.

$$0 = -P + \sum_i m_i e_{f,i} - \sum_e m_e e_{f,e} - E_d \qquad (2)$$

$$e_f = (h - h_o) - T_o(s - s_o) \qquad (3)$$

In exergy analysis, the reference environment is considered to be large, uniform, and have constant intensive properties that are representative of the actual surroundings of the system (Moran and Shapiro, 2000). For this analysis, the dead state was defined in each model run by the average measured wet-bulb temperature and ambient pressure for the steady-state hour being modeled. The wet-bulb temperature was chosen because it is the lowest possible temperature at which evaporative cooling may occur and thus sets the floor on condenser water temperature and condensing pressures. Addi-

tionally, it was found that wet-bulb temperature was the best predictor of evaporator cooling load (Harrell, 2008).

The signage of exergy transfer in Equation 2 is the same as the energy transfer in Equation 1, however the direction of exergy transfer is only the same as the direction of heat transfer if the process temperature exceeds the wet-bulb (dead state) temperature. Thus, while heat energy flows to the evaporator from the cooling coils, exergy flows in the opposite direction, from the evaporator to the cooling coils, because the chilled water temperature is below the ambient wet-bulb temperature.

Exergy transfer into the system with the steam supply and out of the system at the cooling coils and cooling tower was calculated from the net change in flow exergy of the working fluid, with zero exergy destruction. The net change in flow exergy accompanying heat losses from the high pressure steam piping was counted as exergy destroyed because these losses represent avoidable exergy waste.

Cost Modeling

Rational costing of exergy destruction in the system was accomplished by first performing cost balances on all the component and subsystem control volumes. Costs enter the system with the steam supply, cooling tower makeup water, and with electricity used in pumps and fans. Costs are conserved and all accrue toward the cooling coils. Exergy unit costs were calculated by dividing the cost flow rate, C, by the magnitude of the exergy transfer rate, $|E|$, between each component control volume. The exergy unit cost increase due to each component, the *component cost*, c_j, was found according to Equation 4, where cost and exergy transfer were evaluated at the cost exit of each control volume and the component indices, j, were arranged in order of increasing costs. For this analysis, the control volumes were chained from the steam input to the cooling coil such that the final exergy unit cost at the cooling coil was equal to the exergy unit cost of the steam supply plus the sum of all the component costs in the chain. The increases in exergy unit cost at the cooling coils due to the heat rejection subsystem were accounted for in each condenser in proportion to its rate of exergy rejection.

$$c_j = \left(\frac{C_j}{|E_j|}\right) - \left(\frac{C_{j-1}}{|E_{j-1}|}\right) \qquad (4)$$

where $C_j \geq C_{j-1}$.

This method of exergy-based costing is useful because it allows direct comparison of the economic impact of losses throughout the system regardless of their source. Along the path from the steam supply to the delivery of chilled water to the coils, exergy is continually destroyed while costs continually increase, making the remaining exergy more and more valuable. Thus, for example, the exergy of the pumping power input to the chilled water loop has little value compared to the flow exergy of the chilled water being distributed, which embodies all the exergy destruction and cost inputs upstream in the system.

RESULTS

The rate balance model was executed as a system of simultaneous equations, which yielded a complete inventory of all steady-state energy, exergy, and cost transfers across each component boundary. A model run was performed for each chiller (West and South), and for each hour where the input data set passed the tests previously described. First, the results for a particular model run are described in detail, followed by a comparison of results across a range of load conditions.

Figure 3 shows the relative magnitude and direction of the (a) energy, (b) cost, and (c) exergy flows between subsystems for the West chiller operating at 70% of rated evaporator load. Each subsystem is represented by a dashed box and labeled with the abbreviations: chilled water distribution (*chw*), refrigeration (*ref*), steam turbine drive (*stm*), and heat rejection (*reject*). Table 3 lists the maximum transfer rates in the system for energy, cost, and exergy; the transfer rates at each location numbered in Figure 3 are listed relative to these maximum values. The total exergy destruction at the subsystem level is also listed as a fraction of the maximum exergy transfer rate in Table 3 and is shown in Figure 3 as an open flow path that dissipates within the subsystem boundaries. These results clearly demonstrate the conservation of energy and cost within the system; all energy inputs combine and exit through the cooling tower (except for steam losses), and all cost inputs combine and exit through the cooling coils, the point of use. The cooling tower, point 8, is of particular interest. The large heat rejection rate has no recoverable monetary value and a small exergy

transfer to the environment due to the close approach of the cooling tower exit water temperature and the ambient wet-bulb temperature. In the limit that these two temperatures were equal, the exergy transfer would be zero by the definition of the dead state and there would be no available energy to drive the evaporative cooling of the condenser water. On the other side of the system, the cooling coils see the maximum cost rate, but only a small fraction of the original exergy input remains as a useful output. Figure 3 (c) clearly shows most of the exergy is destroyed within the steam turbine drive and refrigeration subsystems. Additionally, the exergy inputs for fluid transport at points 6 and 10 are completely dissipated by fluid friction.

Figure 4 highlights the importance of using exergy-based cost accounting in order to determine the true economic impact of losses distributed throughout the system. The two pie charts represent the total exergy destruction and the total exergy unit cost increase in the chilled water distribution subsystem for the West chiller at 70% load. Each is divided into the relative contributions from each of the five components within the subsystem, three pump sets and two open bypasses. Comparing the two pie charts shows that while the bypasses together account for only 19% of the exergy destroyed, they cause 58% of the cost increase.

This discrepancy arises because the mixing in the bypasses destroys exergy that embodies all the costs accumulated upstream in the system, while the dissipation due to fluid friction from pumping embodies only the electricity costs input to the pumps themselves. The following sections describe the results for selected runs over a range of evaporator
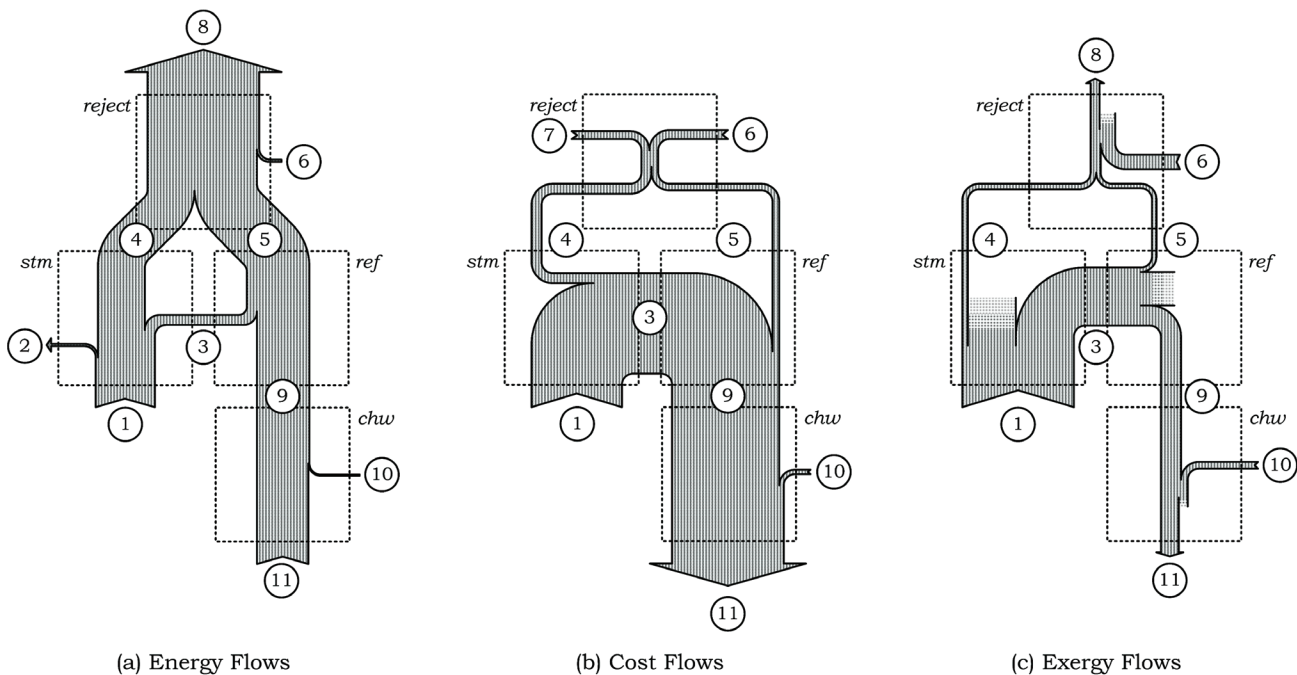

(a) Energy Flows   (b) Cost Flows   (c) Exergy Flows

Figure 3   *Comparison of energy, cost, exergy transfer, and exergy destruction rates for the west chiller at 70% load.*

Table 3. Maximum and Relative Energy, Cost, Exergy Transfer, and Exergy Destruction Rates for the West Chiller at 70% Load

		Energy	Cost	Exergy
Maximum Transfer Rates:		**18,093 kW**	**$343.12/h**	**2,972 kW**
Point	**Transfer Location**	**Relative Transfer Rates**		
1	Steam Supply	53%	81%	100%
2	Steam Losses	2%	---	---
3	Turbine/Compressor Shaft	9%	90%	52%
4	Steam Surface Condenser	42%	9%	5%
5	Refrigerant Condenser	56%	6%	4%
6	Tower Fans + Condenser Loop Pumps	2%	8%	13%
7	Tower Water Cost	---	7%	---
8	Heat Rejected to Atmosphere	100%	---	8%
9	Evaporator	47%	96%	18%
10	Chilled Water Loop Pumps	1%	4%	6%
11	Cooling Coils	46%	100%	16%
	Subsystem	**Relative Exergy Destruction Rates**		
reject	Heat Rejection Subsystem	---	---	14%
stm	Steam Turbine Drive Subsystem	---	---	42%
ref	Refrigeration Subsystem	---	---	31%
chw	Chilled Water Distribution Subsystem	---	---	8%

■ Primary Loop Pumps
▨ Distribution Loop Pumps
▢ Building Loop Pumps
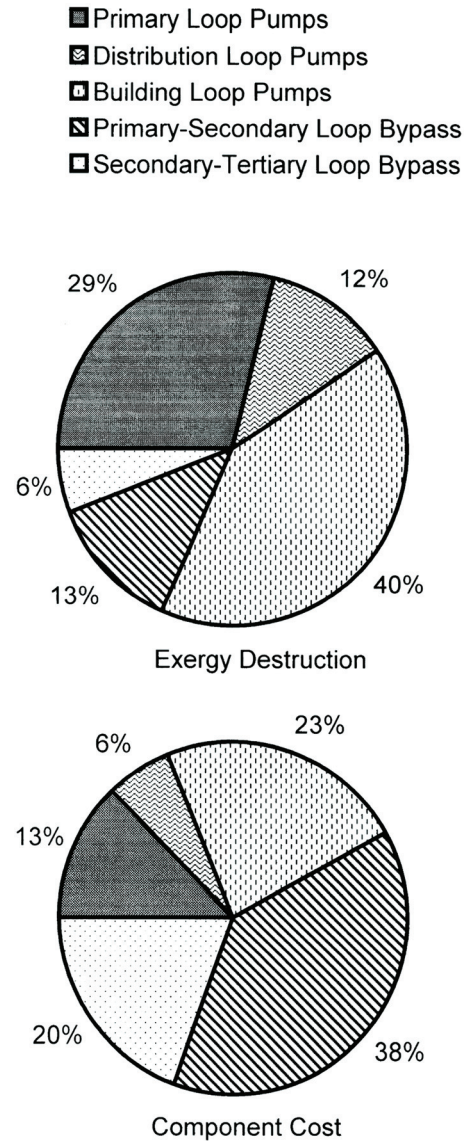◪ Primary-Secondary Loop Bypass
▢ Secondary-Tertiary Loop Bypass

Figure 4 Relative share by component of exergy destruction and component cost for the chilled water distribution subsystem of the West chiller at 70% load.

loads for both chillers so that the effects of loading can be seen on the exergy destruction rates, exergetic efficiencies, relative component costs, and subsystem exergy output. Component costs are displayed in relative terms for clarity because the absolute exergy unit costs vary widely. Low evaporator loads typically correspond to low wet-bulb temperatures and thus low exergy output, which causes exergy unit costs to spike.

Overall Chiller System

Figure 5 shows the exergetic efficiency, determined by Equation 5, and compares the exergy destroyed of the four subsystems of the West chiller and includes motor efficiencies, which previously were not included. The steam drive subsystem had the greatest exergy destroyed and remained

relatively constant at all cooling rates. The second most exergy destroyed occurred in the refrigeration subsystem; the exergy destruction noticeably increased as cooling rate increased. The overall chiller system exergetic efficiency increased with the cooling rate but remained quite low, ranging from only 3% to 13%. Figure 6 shows the relative costs of the exergy destroyed in the four subsystems of the West chiller. The chilled water distribution subsystem contributed the greatest cost at low cooling loads whereas the refrigeration subsystem generated the greatest unit cost increase at high cooling loads. The constant exergy unit cost of the steam supply is also shown and its reduced influence at low loads demonstrates how the
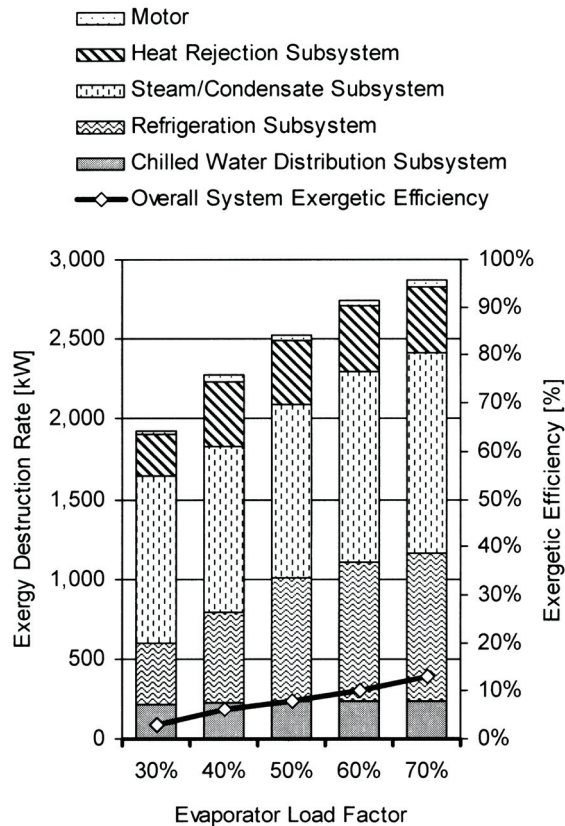
Figure 5 *Exergy destruction rate of all subsystems and exergetic efficiency of the overall West chiller system.*
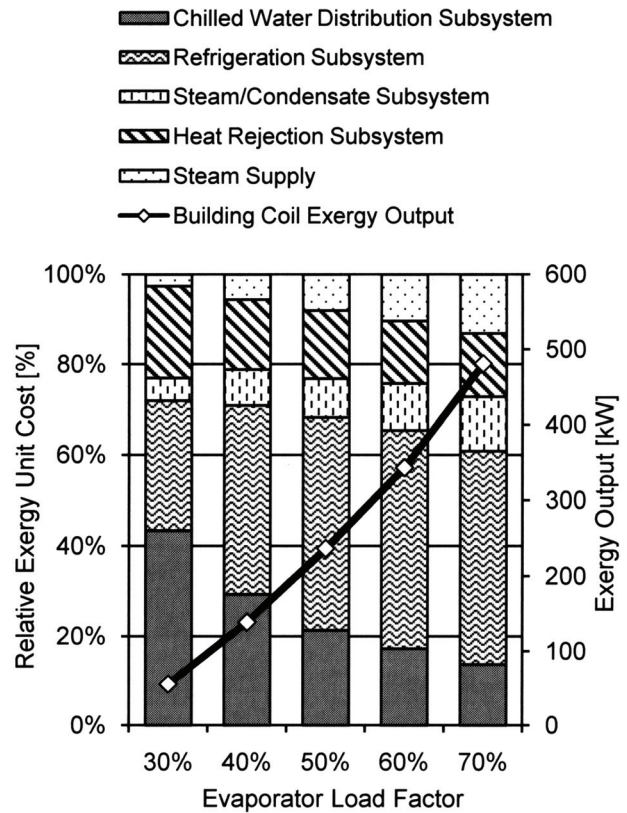

Figure 6 *Relative exergy unit cost of all subsystems and exergy output of the overall West chiller system.*

exergy unit cost increases due to exergy destruction in the subsystems escalate at low loads when the wet-bulb temperature drops closer toward the chilled water temperature.

$$\eta_{x,sys} = \frac{E_{f,coil}}{E_{f,stm} + P_{elec}} \qquad (5)$$

Chilled Water Distribution Subsystem

Figure 7 shows the exergy destruction due to each modeled component in the chilled water distribution subsystem: the primary, distribution, and building pumps, the primary-secondary bypass, and the secondary-tertiary bypass. Exergy destroyed in the constant speed primary and building pumps was most significant, while the distribution pumps operating at reduced speed showed lower losses. Exergy destruction due to mixing in the bypasses was also significant. The exergetic efficiency of the chilled water distribution subsystem, defined by Equation 6, is greater than 60% during higher loads but is very low at part load conditions. This change is explained by a relatively constant rate of exergy destruction due to constant speed pumping, but a falling rate

of exergy delivery as the wet-bulb temperature drops toward the chilled water temperature at part load.

$$\eta_{x,chw} = \frac{E_{f,coil}}{E_{f,evap} + \sum P_{pumps}} \qquad (6)$$

Figure 8 illustrates the economic impact of the exergy destroyed in each component relative to the total impact of the subsystem on the final exergy unit cost at the cooling coil. Since exergy decreases throughout the subsystem, exergy destruction near the end of the subsystem when less exergy exists has a larger unit cost impact. The cost of exergy destruction due to mixing in the bypasses is more significant than the cost of pumping and the significance increases as the total exergy delivered decreases at part load. The rate of exergy output to the cooling coils is shown as a reference.

Refrigeration Subsystem

Figure 9 shows the exergy destruction rates of the components of the refrigeration subsystem: the evaporator, compressor, condenser, and throttling valve, along with the exergetic efficiency of the subsystem as defined by Equation 7. The compressor is the dominant and relatively constant source of
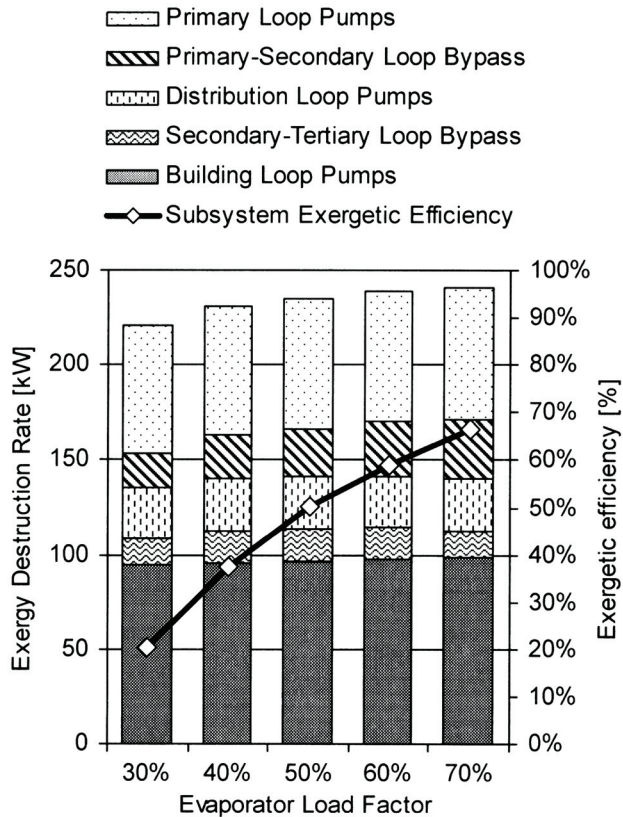
Figure 7 *Exergy destruction rate of components and exergetic efficiency of the chilled water distribution subsystem of the West chiller.*

Figure 8 *Relative exergy unit cost of components and exergy output of the chilled water distribution subsystem of the West chiller.*

irreversibility in the refrigeration subsystem. The rates of exergy destruction in the other components are nearly proportional to the load and are associated with increasing refrigerant flow. Exergy destruction in the heat exchangers is due to heat transfer through a finite temperature difference while exergy destruction in the compressor and valve are due to fluid friction. The exergy destruction of the three-pass evaporator of the West chiller, shown elsewhere (Harrell, 2008), is significantly less due to a closer approach temperature than that of the two-pass evaporator of the South chiller, shown here. Exergetic efficiency of the subsystem is poor and fairly constant, ranging between 20% and 30%.

$$\eta_{x,ref} = \frac{E_{f,evap}}{P_{turb}} \qquad (7)$$

Figure 10 shows the relative component costs of the refrigeration subsystem expressed as a percentage of the total subsystem exergy unit cost. While the compressor is the dominant source of exergy destruction, the loss due to finite-rate heat transfer in the evaporator is the dominant cost in the subsystem. The cost imported from the heat rejection subsystem is the second largest, increasing in relative importance
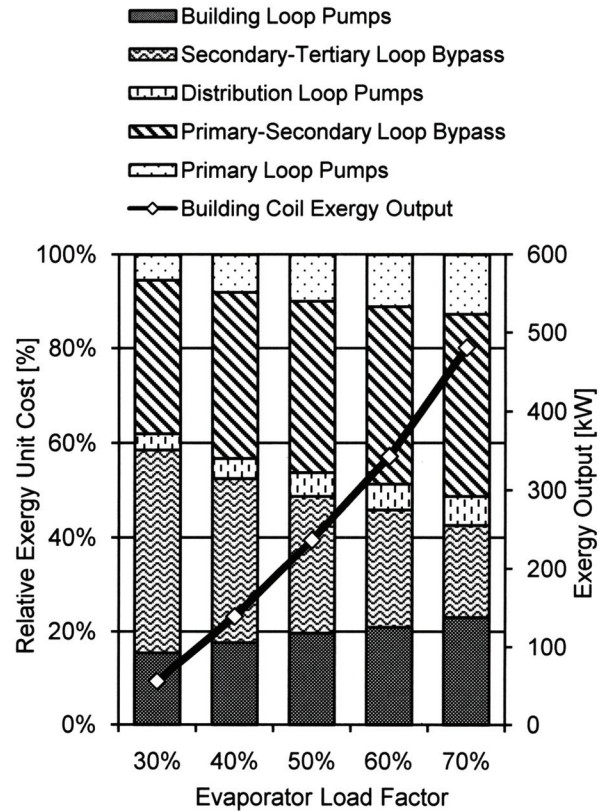
with decreasing load. The exergy output of the subsystem at the evaporator is shown as a reference.

Steam Turbine Drive Subsystem

Figure 11 illustrates the exergy destruction rates and exergetic efficiency of the steam turbine drive subsystem of the South chiller. The steam turbine is clearly the greatest source of irreversibility followed by the losses from the high pressure steam piping due to inadequate insulation. The exergetic efficiency, defined by Equation 8, ranges from 36% to 48%. The erratic nature of the data may have resulted from the necessity of using a single point measurement of the steam mass flow rather than an hourly mean of at least ten measurements.

$$\eta_{x,stm} = \frac{P_{turb}}{E_{f,stm} + P_{hwp}} \qquad (8)$$

Figure 12 shows the component costs relative to the total exergy unit cost of the steam turbine drive subsystem. Again, the turbine losses clearly dominate at approximately 60% of the total, with the cost of heat rejection from the surface condenser representing 15% to 20%, depending on load. Heat losses represent about 5% to 10% of the subsystem costs. The
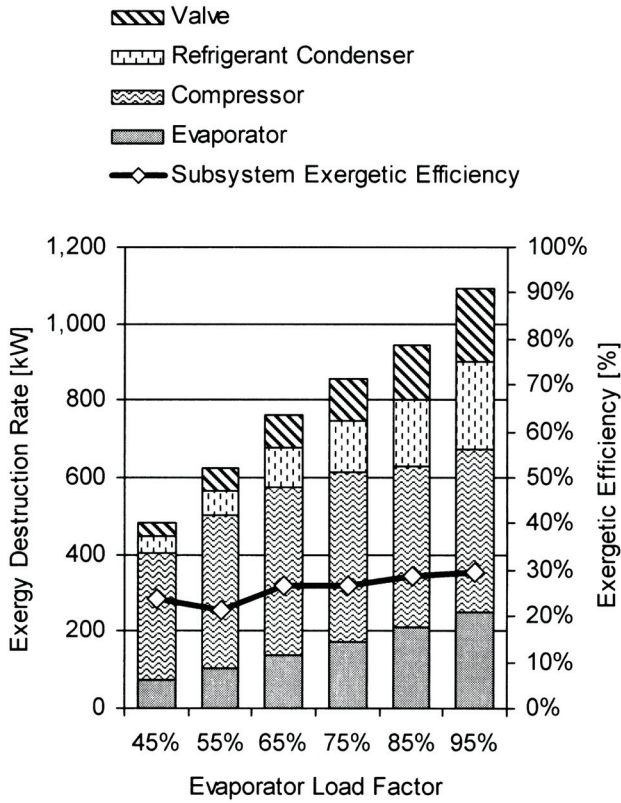
Figure 9 *Exergy destruction rate of components and exergetic efficiency of the refrigeration subsystem of the South chiller.*
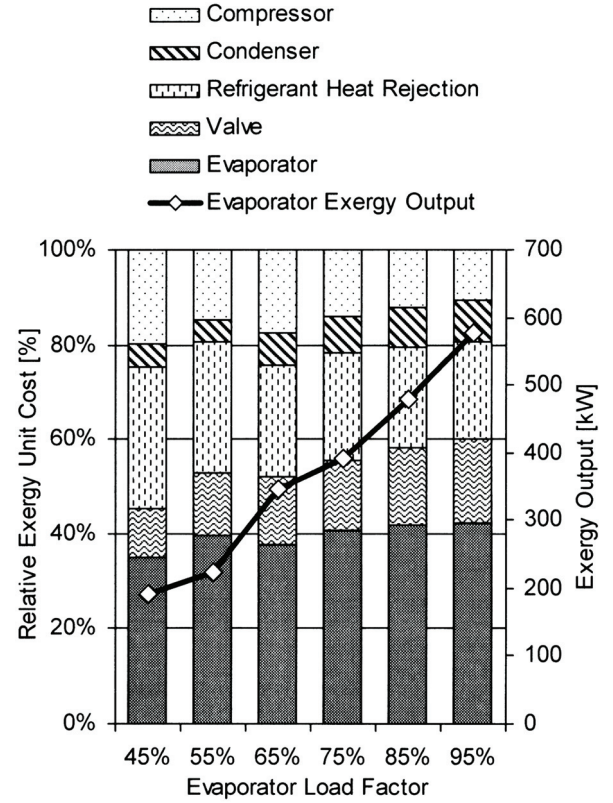

Figure 10 *Relative exergy unit cost of components and exergy output of the refrigeration subsystem of the South chiller.*

subsystem exergy output in terms of turbine power is shown as a reference.

Heat Rejection Subsystem

Exergy destruction rates and the exergetic efficiency of the heat rejection subsystem of the West chiller system were calculated and are shown elsewhere (Harrell, 2008). The constant rate of exergy destruction from the condenser water pumps is evident and a sharp reduction in fan power is evident at the lowest cooling capacity, when the cooling tower fans run at half speed due to a low wet-bulb temperature. At this condition, exergy destruction due to mixing at the cooling tower bypass is also evident indicating that some controls tuning may be needed so that the fans are completely off before the bypass valve opens. Exergetic efficiency, found using Equation 9, was at its highest, 39%, when the fans were at part speed.

$$\eta_{x,reject} = \frac{E_{f,reject}}{E_{f,scnd} + E_{f,cond} + P_{cwp} + P_{ctf}} \qquad (9)$$

DISCUSSION

These results show the utility of exergy analysis and especially exergy-based cost accounting for indentifying and rank-

ing the major sources of inefficiency and cost in thermal systems. Unlike energy, exergy is a non-conserved quantity and is lost as the system state falls closer to that of the reference environment, or dead state. The available work potential is destroyed through spontaneous and irreversible processes such as friction, non-isentropic expansion and compression, heat transfer over a finite temperature difference, and mixing. As highlighted in Figures 3 and 4, exergy analysis provides information about the internal losses of real processes that energy and cost analysis alone cannot. Exergy-based cost accounting is important in order to account for the effects of compounding losses as exergy is dissipated along the path to the system's intended useful output. This compounding effect increases the effective cost of incremental exergy destruction closer to the system output. In addition, exergy analysis allows for direct comparison of losses and efficiencies across different subsystems such as power and refrigeration cycles, where thermal efficiency and coefficient of performance metrics from energy analysis are not directly comparable.

The reference environment concept in exergy analysis is useful for systems such as power and refrigeration cycles that reject heat to the environment; however, the choice of the dead state has a profound effect on the results. A dead state defined
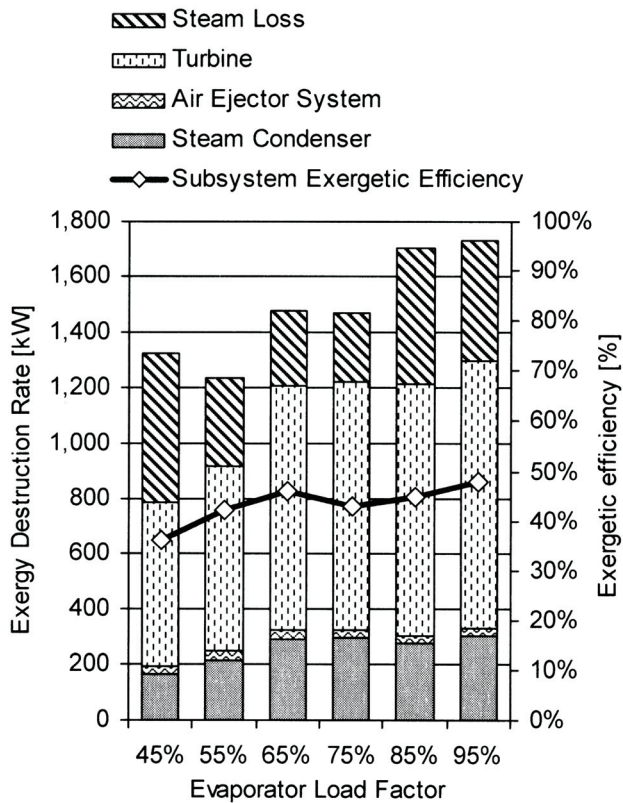
Figure 11 *Exergy destruction rate of components and exergetic efficiency of the steam turbine drive subsystem of the South chiller.*
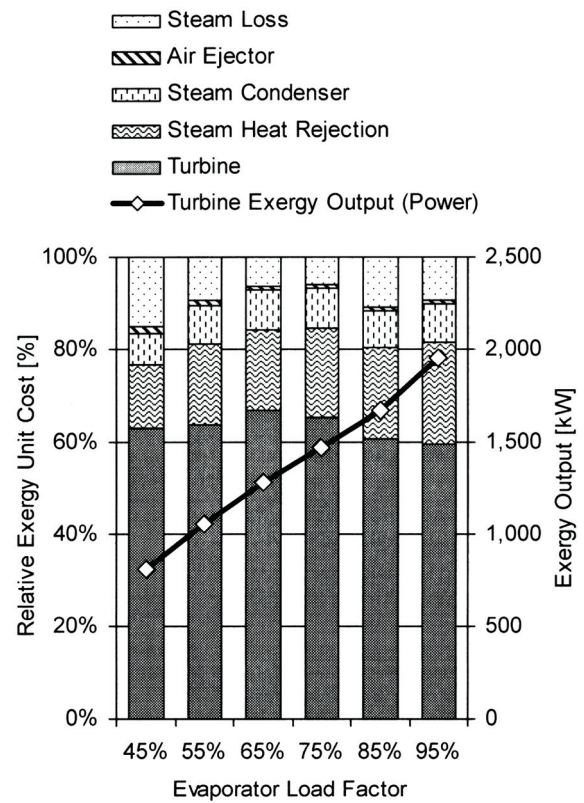

Figure 12 *Relative exergy unit cost of components and exergy output of the steam turbine drive subsystem of the South chiller.*

by atmospheric pressure and wet-bulb temperature is a logical choice for a refrigeration system with evaporative heat rejection. On the heat rejection side, the wet-bulb temperature defines the lower limit for the condenser water temperature and on the cooling coil side, the wet-bulb temperature defines the upper limit on chilled water supply temperature in order to provide useful cooling. If the chilled water temperature is above the wet-bulb temperature, more cooling could be achieved with an air-side economizer and direct evaporative cooling than with a cooling coil.

CONCLUSIONS AND RECOMMENDATIONS

This paper presents data collected from a central chilled water system. The data was modeled using steady-state, control-volume, rate balances for mass, energy, exergy, and cost flows. The results from these models point to a number of key opportunities for increasing the capacity and reducing utility costs of the central chilled water system. Also, the data collection, modeling, and trends of the results are applicable to many other central chilled water systems and provide areas for operators of other systems to study. Examining the results of the exergetic analysis, the following improvements are suggested.

1. Install VFDs on all building pumps to reduce or eliminate the exergy destruction due to mixing at the building bypasses during part load conditions. This will bring colder water into each building allowing more cooling capability from the chiller system and reducing moisture issues in the buildings that have been reported. The VFDs will also reduce electric usage of the motors during part load conditions. This recommendation is critical for increasing cooling capacity utilization of the chiller systems and is expected to be relatively cost-effective to complete. Given the high cost of chilled water production, it is imperative that the chilled water distribution subsystem deliver exergy from the evaporator to the cooling coils with a minimum of losses. Therefore, this modification is needed regardless of any other improvements made.

2. The exergetic efficiency increased as load increased, therefore at the beginning and end of the cooling season when there are light cooling loads, operate the entire campus with only one chiller system. One chiller can serve the entire campus by opening the system isolation valve which connects both chilled water distribution loops together.

3. During high load conditions operate the third primary loop pump to increase flow through the evaporator. This will reduce the exergy destruction associated with heat transfer in the evaporator by reducing the approach of the refrigerant and chilled water temperatures. This measure is especially recommended for the two-pass evaporator of the South chiller where exergy destruction of the evaporator was second in magnitude after the exergy destruction of the compressor.

4. Control the chiller capacity more aggressively with compressor speed as opposed to relying on the inlet guide vanes. The compressor and steam turbine maintain a relatively constant rate of exergy destruction due to fluid friction by operating at a nearly-constant high speed. Using speed control as the primary means of capacity modulation will allow operation at lower speeds, reducing friction losses in both the refrigeration and steam turbine subsystems. Inlet guide vanes could be used primarily for anti-surge stability control after the compressor and turbine have been reduced to lowest appropriate speed.

5. Better insulate steam piping to reduce the steam condensate and exergy destroyed due to unintended heat losses ahead of the turbine.

6. Consider replacing the steam turbine with a variable speed motor. This change will greatly facilitate speed control and eliminate all the exergy destroyed in the steam subsystem. However, an entire campus evaluation is needed to determine the interactions of this modification with other campus systems, especially boiler plant operations.

NOMENCLATURE

C = cost rate [$/hr]
c = exergy unit cost [$/MJ]
COP = coefficient of performance [-]
E = exergy rate [kW]
e = specific exergy [kJ/kg]
h = specific enthalpy [kJ/kg]
m = mass flow rate [kg/s]
P = power [kW]
q = heat transfer rate [kW]
s = specific entropy [kJ/kg K]
T = absolute temperature [K]
t = temperature [°C]
VFD = variable frequency drive [-]
Δp = pressure difference [kPa]
η = efficiency [-]
Σ = sum [-]

Subscripts

BS = building supply (applied to chilled water temperature at buildings)

chw = chilled water distribution subsystem
$coil$ = building coil
$cond$ = refrigerant condenser
ctf = cooling tower fan
cwp = condenser water pump
d = destruction (applied to exergy)
e = exit
$elec$ = electrical
$evap$ = refrigerant evaporator / water cooler
f = flow (applied to exergy)
hwp = condensate hotwell pump
i = inlet
j = component index
LR = loop return (applied to chilled water temperature at buildings)
LS = loop supply (applied to chilled water temperature at buildings)
o = ambient or dead state condition
ref = refrigerant, refrigeration subsystem
$reject$ = heat rejection subsystem
$scnd$ = steam (surface) condenser
stm = steam/condensate, steam/condensate subsystem
sys = entire system
$turb$ = turbine
x = exergetic

REFERENCES

ARI. 2003. 2003 standard for performance rating of water-chilling packages using the vapor compression cycle: standard 550/590. Air-Conditioning & Refrigeration Institute, Arlington, VA, p. 18, Sect. C6.2.

Braun, J.E., S.A. Klein, W.A. Beckman, and J.W. Mitchell. 1989. Methodologies for optimal control of chilled water systems without storage. ASHRAE Transactions 95(1):652-662.

Gordon, J.M. and K.C. Ng. 2000. Cool thermodynamics: the engineering and physics of predictive, diagnostic, and optimization methods for cooling systems. Cambridge International Science Publishing, Cambridge, UK.

Harrell, J.M. 2008. Improving efficiency in the SIUC campus chilled water system using exergy analysis. Masters thesis, Southern Illinois University, Carbondale.

Hartman, T. 2001. Ultra-efficient cooling with demand-based control. Heating/Piping/Air Conditioning Engineering 73(12):29-35.

Hyman, L.B. and D. Little. 2004. Overcoming low delta t, negative delta p at a large university campus. ASHRAE Journal 46(2):28-34.

Klein, S.A., D.R. Nugent, and J.W. Mitchell. 1988. Investigation of control alternatives for a steam turbine driven chiller. ASHRAE Transactions 94(1):627-643.

Moran, M.J. and H.N. Shapiro. 2000. Fundamentals of engineering thermodynamics fourth edition. John Wiley & Sons, Inc., New York.

Rosen, M.A. and I. Dincer. 2004. A study of industrial steam process heating through exergy analysis. International Journal of Energy Research 28(10):917-930.

Rosen, M.A., M.N. Le, and I. Dincer. 2004. Exergetic analysis of cogeneration-based district energy systems. Journal of Power and Energy 218(6):369-375.

Taylor, S.T. 2002. Degrading chilled water plant delta-t: causes and mitigation. ASHRAE Transactions 108(1):1-13.